Research article

Unveiling the gut microbiota and metabolite profiles in guinea pigs with form deprivation myopia through 16S rRNA gene sequencing and untargeted metabolomics

Yajun Wu [a,b,c,#], Hua Fan [d,#], Yuliang Feng [a,b,c], Jiasong Yang [a,b,c], Xiaobo Cen [e,**], Wensheng Li [a,b,c,*]

[a] Aier Academy of Ophthalmology, Central South University, Changsha, Hunan, 410000, China
[b] Department of Ophthalmology, Shanghai Aier Eye Hospital, Shanghai, 200235, China
[c] Shanghai Aier Eye Institute, Shanghai, 200235, China
[d] Shanxi Aier Eye Hospital, Taiyuan, Shanxi, 030000, China
[e] WestChina-Frontier PharmaTech Co., Ltd, Chengdu, Sichuan, 610000, China

ARTICLE INFO

ABSTRACT

Aim: The aim of this study was to confirm the presence of the form deprivation myopia (FDM) guinea pig eye-gut axis and investigate the relationship between serum vasoactive intestinal peptide (VIP), lipopolysaccharides (LPS), specific gut microbiota and their metabolites.
Method: 20 specific-pathogen-free (SPF) guinea pigs were divided into the FDM and the control (Con) group. Following model induction, serum levels of VIP and LPS were quantified. A combination of 16S ribosomal ribosomal Ribonucleic Acid (rRNA) gene sequencing, non-targeted metabolomics and bioinformatics analysis were employed to identify disparities in gut microbiota and metabolites between the two groups of guinea pigs.
Result: Compared to the control group, FDM guinea pigs exhibited a significant trend towards myopia, along with significantly elevated concentrations of LPS and VIP ($p < 0.0001$). Furthermore, Ruminococcus_albus emerged as the predominant bacterial community enriched in FDM ($p < 0.05$), and demonstrated positive correlations with 10 metabolites, including L-Glutamic acid, Additionally, Ruminococcus_albus exhibited positive correlations with VIP and LPS levels ($p < 0.05$).
Conclusion: The findings suggest that the Ruminococcus_Albus and glutamate metabolic pathways play a significant role in myopia development, leading to concurrent alterations in serum VIP and LPS levels in FDM guinea pigs. This underscores the potential of specific gut microbiota and their metabolites as pivotal biomarkers involved in the pathogenesis of myopia.

1. Introduction

The microbiota plays a vital role in maintaining the digestive and immune functions of the human body [1]. Disruptions to the

---

* Corresponding author. Aier Academy of Ophthalmology, Central South University, Changsha, Hunan, 410000, China.
** Corresponding author.
 E-mail addresses: xbcen@scu.edu.cn, xbcen@glpcd.com (X. Cen), drlws@qq.com, liwensheng@aierchina.com (W. Li).
Co-first authors

microbiota can lead to bodily imbalances and the onset of diseases [2]. Notably, the gastrointestinal tract hosts up to 95% of the human body's microbiota [3], highlighting the importance of gut microbiota stability for human health. Similarly, mammals harbor a diverse array of microbiota in the gastrointestinal tract, comprising bacteria, archaea, fungi, protozoa, and viruses [4]. Besides their roles in digestion and immunity, these microbiota also contribute to the regulating the host's endocrine and nervous systems [5], categorized by kingdom, phylum, class, order, family, genus, and species. In recent years, disruptions to gut microbiota have been associated with neurological and eye diseases [6–8], indicating the existence of the gut-brain axis and the gut-eye axis. This understanding opens new avenues for comprehending disease pathogenesis and treatment.

Sjogren's syndrome (SS), a chronic autoimmune disease, can lead to severe dry eye, with disruptions in gut microbiota associated with immune dry eye [9]. Treatments utilizing a mixture of Saccharomyces boulardii MUCL 53837 and Enterococcus faecium LMG S-28935 have demonstrated efficacy in alleviating dry eye syndrome [10]. Similarly, autoimmune uveitis has been linked to gut microbiota disorders, with decreased concentrations of secondary bile acids mediated by gut microbiota observed in affected animals [11]. Probiotic treatments have shown potential in reducing uveitis severity [12]. Additionally, conditions such as diabetic retinopathy [13], glaucoma, and age-related macular degeneration have established connections with the gut-eye axis [14]. Apart from the gut-eye axis, bidirectional communication between the brain and intestines via gut microbiota is essential [15]. The role of the gut-brain axis in neurological and psychiatric disease occurrence and development is an ongoing area of research. For instance, in Parkinson's disease (PD), a common central nervous system disorder, alterations in gut microbiota producing short-chain fatty acids have been noted [16]. Similarly, Alzheimer's disease (AD), the most common form of dementia, is associated with dysbiosis of the microbiota, contributing to increased gut and blood-brain barrier permeability and participating in the onset of AD and other neurodegenerative diseases [17]. This wide-ranging involvement of gut microbiota suggests its significant role in the pathogenesis of certain eye and brain-related diseases.

Myopia, a prevalent ophthalmic disease causing global visual impairment [18], is also considered a neurodegenerative disease, particularly high myopia and pathological myopia [19]. Despite extensive research, the complete pathogenesis of myopia remains elusive. Previous research [20] from our group identified an association between gut microbiota imbalance and the retina. We observed a positive correlation between retinal inflammatory factor levels and microbiota metabolites, specifically lipopolysaccharides (LPS), and a negative correlation with short-chain fatty acids. Notably, myopia, especially high myopia, exhibits significant retinal degenerative changes such as retinal sclera thinning, optic disc deformation, perioptic disc atrophy, and choroidal atrophy. Additionally, given that myopia is not only a retinal disease but also a brain disease, closely related to the central nervous system and associated with certain neurodegenerative system diseases, such as PD patients exhibiting not only nervous system symptoms but also a wide range of visual impairments [21]. Our previous research [22] used MRI to reveal decreased cerebral cortex thickness in myopic patients, akin to PD patients who also exhibit widespread cortical thinning [23]. Given PD's close association with gut microbiota disorders and myopia sharing similar mechanisms with neurological diseases, we speculate whether myopia is also associated with gut microbiota disorders, particularly its connection with LPS.

Moreover, vasoactive intestinal peptide (VIP), a 28-amino-acid peptide initially isolated from pig intestines for its ability to dilate small arteries [24]. has been confirmed by Bains et al. [25] to be important in establishing and maintaining gut microbiota. Through 16S ribosomal RNA (rRNA) gene sequencing on the feces of VIP −/− knockout mice, significant changes in fecal bacterial composition and biodiversity, along with decreased weight, were observed compared to normal mice, highlighting the critical role of VIP in maintaining mouse gut microbiota stability and weight. Additionally, VIP is not only involved in the gastrointestinal system but also serves as a neuromodulator in the eyes [26]. Despite its implication in the pathological and physiological changes of myopia [27], the impact and specific mechanism of VIP in myopia remain controversial. VIP's close association with both gut microbiota and myopia raises intriguing questions, however, current research lacks evidence regarding the impact of gut microbiota on myopia's pathophysiology and the relationship between VIP, gut microbiota, and myopia.

To address these gaps, our study utilized enzyme-linked immunosorbent assay (ELISA) to measure serum VIP and LPS levels in guinea pigs with form deprivation myopia (FDM). This was complemented with 16S rRNA gene sequencing and untargeted metabolomics to investigate the gut-eye axis in myopia. Bioinformatics analyses were conducted to explore correlations among the identified biomarkers, shedding light on whether gut microbiota and its metabolites are pivotal influencers in myopia's mechanism. This endeavor aims to elucidate the molecular mechanisms of myopia, providing a critical theoretical foundation for its clinical prevention and treatment.

2. Methods

2.1. Experimental animals

Twenty healthy 3-week-old specific-pathogen-free (SPF) guinea pigs, weighing between 100 and 160g (individual values within ±20% of the mean), were included. To mitigate potential differences in eye size, axial length (AL), and refractive error (RE) due to gender variance in young guinea pigs, male guinea pigs with larger body size and eyeballs were uniformly selected compared to females of the same age. All guinea pigs, were randomly assigned to either the blank control group (Con) or the form deprivation myopia group (FDM), with 10 guinea pigs in each group. In the FDM group, the eye was designated as the myopia groupl. The guinea pigs were procured from Beijing Weitonglihua Experimental Animal Technology Co., Ltd. (production license No.:SCXK (Beijing) 2021-0011). Throughout the study, the guinea pigs were housed in an SPF environment, maintaining a room temperature range of 18~29 °C (daily temperature difference ≤4 °C), relative humidity of 40~70%, and artificial lighting with a 12/12 h day-night cycle. They had ad libitum access to food and water during the experimental period.

Con Group:No treatment was administered to the eyes of the control group. FDM Group: The eyes of guinea pigs in the FDM group were covered with a non-toxic, white No.6 latex balloon, ensuring that neither the cornea nor the eyelid of the eye experienced compression. Diopter (D), AL, and vitreous cavity depth were measured for all guinea pigs before and 4 weeks after the experiment. The success of the model was confirmed by observing an increase in the AL and vitreous cavity depth of the eyes, along with a decrease in RE in the FDM group. Guinea pigs exhibiting eye diseases, anisometropia exceeding 1.50D, and pre-existing myopia were excluded from the experiment.

After the experiment, all guinea pigs were euthanized by intramuscular injection of 2 mg/kg diazepam, followed by intravenous injection of pentobarbital sodium (30 mg/kg), and ultimately by abdominal arterial bleeding.

This study received ethical approval from the Shanghai Aier Eye Animal Ethics Committee (No. SHAIER2023YN002), all animals in this study were approved by the Institutional Animal Care and Use Committee (IACUC) of WestChina-Frontier Pharma Tech Co., Ltd. (Approval Number: IACUC- SW-S2023023-P001-02), and comply with Animal Research: Reporting in Vivo Experiments (ARRIVE) guidelines.

2.2. Measurement of ophthalmic parameters

AL and vitreous cavity depth were assessed using the OD-1 A-scan device (Kaixin, Xuzhou, China). Guinea pigs were subjected to topical anesthesia with 1–2 drops of oxybuprocaine hydrochloride eye drops on the binocular surface. The procedure was repeated 2–3 times with a 5-min interval, and the disappearance of the corneal reflex served as the standard. The probe was aimed at the pupillary region of the guinea pigs, gently touching the cornea without applying pressure. Values for AL and vitreous cavity depth were read, and each eye was measured three times, with the average value recorded.

RE was determined using a small animal infrared refractometer (photorefractor, Sriatech GmbH, Germany). Guinea pigs were positioned in a dark and quiet environment, and the camera was focused on the pupil. The eye position of the guinea pig was stabilized, and the RE readings were recorded once they reached stability.

All measurements were conducted by an experienced experimenter.

2.3. Detection of serum VIP and LPS levels

Guinea pigs were anesthetized with 2.5% pentobarbital (25 mg/kg), and 2 mL of blood was collected from the dorsal veins of the feet. Following centrifugation at 1000 r/min for 20 min, serum and red blood cells were separated, and the supernatant was extracted. Guinea pig VIP Elisa kit and guinea pig LPS Elisa kit provided by Shanghai Kanglang Biotechnology Co., Ltd. were used to detect serum VIP and LPS levels, respectively.

For the assay, the standard product was appropriately diluted, and the procedure included setting a blank well, sample measurement well, and standard well. Sample addition was followed by incubation at 37 °C for 30 min, with thorough washing afterward. Subsequently, 50 µl of enzyme-labeled reagent per well (excluding the blank well) was added, followed by additional incubation and washing steps. Color developer A (50 µl per well) and color developer B (50 µl) were sequentially added, and after a 10-min incubation, termination solution was introduced to halt the reaction (changing from blue to yellow). Finally, the absorbance (OD) value was measured using an enzyme-labeled instrument at a wavelength of 450 nm, and the concentrations of VIP and LPS in the serum of each guinea pig were calculated.

2.4. 16S ribosomal Ribonucleic Acid (rRNA) gene sequencing and bioinformatics analysis of gut microbiota

2.4.1. 16Sr RNA gene sequencing
Fecal samples from all guinea pigs in an SPF environment were collected using a sterile metabolic cage. Upon collection, feces were immediately transferred into sterile centrifuge tubes using sterile forceps and rapidly frozen with liquid nitrogen. Samples were then stored at −80 °C for testing. For library preparation and high-throughput sequencing, of the 16S rRNA gene was employed to characterize the bacterial community. Stool genomic DNA was extracted using the QIAamp DNA Stool Mini Kit (Qiagen, Hilden, Germany). The purity of nucleic acids was assessed using a UV spectrophotometer, and integrity was verified through agarose gel electrophoresis. The v3-v4 region of the bacterial 16S rRNA gene was amplified using primers (357F 5′-ACTCCTACGGGRAGGCAGCAG-3′ and 806R 5′-GGACTACHVGGGTWTCTAAT-3′). After PCR amplification, purified products were recovered using the AxyPrep DNA Gel Recovery Kit (Axygen, USA) and subjected to detection and purification via agarose gel electrophoresis. Sequencing was performed using Illumina Miseq at Microbased Biotechnology (Shanghai) Co., LTD.

2.4.2. Microbiological analysis
For sequence analysis, PE reads obtained from sequencing were initially distinguished by barcode, followed by sequence quality control and filtration. Sequence overlap-based splicing was performed, followed by additional quality control and filtration using Trimmomatic (version 0.38)., Operational taxonomic units (OTUs) were clustered and classified into phylum, class, order, family, genus, and species. USEARCH (version: 8.1.1861) was utilized to cluster the concatenated sequences into OTUs. The specific methods are as follows: 1. the representative sequence of OTU was obtained by clustering with 97% similarity. 2. The chimera generated by PCR amplification was removed from the OTU representative sequence; 3. Use the usearch_global method to compare all sequences back to the OTU representative sequence to obtain the abundance table of each sample in each OTU; 4. After receiving the OTU representative sequence, classify the OTU representative sequence with the database by mothur (classify.seqs) software (version:1.39.5) for species

annotation. The confidence threshold is set to 0.6, and the comparison database is 16S (bacteria):Silva128 (default), Greengene, RDP; 5. Filter the annotated results as follows: A: remove OTUs without annotated results, B: Remove annotated results do not belong to the species in the analysis item. 6. Use the remaining OTU for post-analysis.

Extract information from the OTU comprehensive classification results at six levels: phylum, class, order, family, genus, and species, and calculate the relative abundance percentage of each sample at different classification levels. Statistical analysis at the same classification level included calculation of Shannon, Simpson, Chao, and Ace values under different random sampling conditions using mothur (version 1.39.5) to assess the alpha diversity of gut microbiota in guinea pigs. Data visualization was performed using R software (version 4.3.1, New Zealand) and Origin (version 2022, Originlab, USA).

2.5. Liquid chromatography tandem mass spectrometry (LC-MS) untargeted metabolomics analysis

2.5.1. Metabolite identification

The feces were removed from the $-80\,°C$ refrigerator and thawed slowly on ice. 50 mg samples were taken into a 2 mL centrifuge tube, 800 μL 80% methanol (Sigma Aldrich, Shanghai Aldrich (Shanghai) Trading Co., Ltd.) was added, and the samples were thoroughly mixed by vortex oscillation. Ultrasound at $4\,°C$ for 30 min; Stand at $-40\,°C$ for 1 h, vortex for 30 s, stand at $4\,°C$ for 0.5 h; Centrifuge at $4\,°C$ and 12000 rpm for 15 min; Take all the supernatant in the centrifugal tube and let it stand for 1 h at $-40\,°C$; Centrifuge at $4\,°C$ and 12000 rpm for 15 min; The 200 μL supernatant was removed, the internal standard (0.14 mg/mL dichlorophenylalanine, Shanghai Aladdin Biochemical Technology Co., Ltd) was added to 5 μL, mixed and transferred into the injection vial. Perform metabolomics analysis on the samples extracted from the above steps.

The metabonomic profile of guinea pig feces was determined using ultra-performance LC-MS (Waters, UPLC; Thermo, Q Exactive). Chromatographic separation utilized an Acquity UPLC HSS T3 column (2.1×100 mm, 1.8 μm) under the following conditions: column temperature at $40\,°C$, flow rate set to 0.300 mL/min, and mobile phase consisting of (A) water (with 0.05% formic acid from Shanghai Aladdin Biochemical Technology Co., Ltd.) and (B) acetonitrile (Sigma Aldrich, Shanghai Aldrich (Shanghai) Trading Co., Ltd.). The injection volume was 5 μL, and the autosampler was maintained at $4\,°C$. Mass spectrometry operated in both positive and negative polarity modes. Mass spectrometry detection parameters for positive (POS) mode included a heater temperature of $300\,°C$, sheath gas velocity of 45 arb, auxiliary gas flow rate of 15 arb, tail gas flow rate of 1 arb, electrospray voltage of 3.0 kV, capillary temperature of $350\,°C$, and S-lens RF level of 30%. For negative (NEG) mode, the parameters were similar, with an electrospray voltage of 3.2 kV and an S-lens RF level of 60%. Scanning modes encompassed full scan (m/z 70–1050) and data-dependent secondary mass spectrometry (dd-MS2, TopN = 10) with resolutions of 70,000 (primary mass spectrometry) and 17,500 (secondary mass spectrometry). Collision mode employed high energy collision dissociation (HCD).

2.5.2. Metabolite analysis

Using Thermo Scientific™ Compound Discoverer™ (version 3.3, Thermo Fisher Scientific, USA) was used for peak recognition, filtering, and calibration. The resulting data matrix, comprising mass/nucleus ratio (m/z), retention time (RT), and peak area (intensity), was obtained. Precursor molecules in positive and negative ion modes were exported to Excel for further analysis after normalization of data for comparability across different orders of magnitude. Principal component analysis (PCA) was conducted using Origin (version 2022,Originlab, USA) to observe the separation degree of samples between the groups. The reference material database was searched, and the VIP value of the principal components of the OPLS-DA model, combined with the p-value of the *t*-test, was used to identify differentially expressed metabolites (biomarkers). LDA Effect Size (LEfSe) analysis was performed using Galaxy (https://usegalaxy.org/) to identify species with significant differences in abundance between groups. Metabolic pathways were studied using the MetPA database (www.metaboanalyst.ca) based on the Kyoto Encyclopedia of Genes and Genomes (KEGG) database (https://www.genome.jp/KEGG/pathway.html). Enrichment of different metabolites was analyzed by metabolic pathway.

2.6. Statistical analysis

SPSS 22.6 software was used for statistical analysis. Measurement data were expressed as mean $\pm$ standard deviation (x $\pm$ s), and the *t*-test was used for measurement data. Pearson correlation was used for correlation analysis, with $p < 0.05$ indicating statistically significant differences. Specific statistical analysis methods for microorganisms and metabolites can be found in sections 2.4.2 and 2.5.2.

3. Results

3.1. The ophthalmic parameters of guinea pigs were assessed before and after modeling

After 4 weeks, following the covering of the eyes in the FDM group, the refractive error (RE) changed from 3.08 ± 0.43 D to -3.31 ± 1.78 D. This demonstrated a significant myopic shift compared to the eyes of the Con group (2.45 ± 0.77 D) with a *p*-value of less than 0.0001. The AL and vitreous cavity depth of the eyes in the FDM group were significantly higher than those in the Con group (8.41 ± 0.10 mm vs. 7.95 ± 0.21 mm for AL, and 3.86 ± 0.16 mm vs. 3.42 ± 0.21 mm for vitreous cavity depth, respectively), with $p < 0.0001$. And there was no significant difference in RE, AL and vitreous cavity depth between two groups at 0 week, as illustrated in Table 1.

3.2. Results of serum VIP and LPS in guinea pigs

After 4 weeks, the serum concentration of LPS in the FDM group was 295.6 ± 17.67 ng/L, which was significantly higher than the concentration in the Con group (212.1 ± 21.39 ng/L) with a t-value of 9.52 and $p < 0.0001$ (see Fig. 1A). Additionally, the serum concentration of VIP in the FDM group was 215.3 ± 27.14 ng/L, which was significantly higher than the concentration in the Con group (126.7 ± 19.93 ng/L) with a *t*-value of 8.32 and $p < 0.0001$ (see Fig. 1B).

3.3. Diversity results of gut microbiota in guinea pigs

According to the sequencing results: After quality control, the observed difference in gut microbiota structure between the FDM group and the Con group was not highly significant (see Fig. 2A). However, statistical differences were observed in the Chao1 index and ACE index, indicating that microbial richness at the OTU level in the FDM group is lower than that in the Con group (see Fig. 2B and C, $p < 0.05$). The shared gut microbiota between the two groups totaled 1610, while the FDM group exhibited 201 unique microbiota, slightly lower than the 211 in the Con group (see Fig. 2D). The difference in species diversity between the two groups was not statistically significant (see Fig. 2E and F).

Through LEfSe analysis: Significant differences in Ruminococcus were identified between the FDM group and Con (refer to Fig. 3A and B). Notably, Ruminococcus_albus exhibited significant enrichment in the FDM group. No differences were observed in microbial communities between the two groups at the phylum level. However, at the class, order, family, genus, and species levels, a total of 12 distinct microbial communities were identified, the specific information on the differential gut microbiota was shown in Table 2, and the comparison results of 12 different gut microbiota between the two groups are presented in the supplementary materials. In comparison with the Con group, Ruminococcus, Ruminococcus_albus, and [Clostridium]_papyrosolvens showed an increased abundance in the FDM group. Conversely, nine bacteria of Alphaproteobacteria, Rhodospirillales, Porphyromonadaceae, Butyricimonas, Roseburia, Parabacteroides, Paraprevotella, gut_metagenome, and Parabacteroides_distasonis exhibited down-regulation. It can be seen that Ruminococcus was significantly positively correlated with Ruminococcus-albus, and significantly negatively correlated with Butyrisimonas and gut-metagenome; besides, Ruminococcus-albus was also significantly positively correlated with [Lostridium]_papyrosolvens, and significantly negatively correlated with Porphyromonadaceae and Butyrisimonas. The correlation between the other differential bacterial communities was illustrated in Fig. 3C. Additionally, Fig. 3D and E represent Ruminococcus in the LEfSe analysis. Differential analysis of Ruminococcus_albus between the FDM group and the Con group indicates a significantly higher abundance of these two bacterial groups in the FDM group than in the Con group.

Fig. 4 shows the classification bar charts of gut microbiota at the genus and species levels for two groups of guinea pigs. It can be seen that the FDM group showed a significant increase in Ruminococcus at the genus level (Fig. 4A) and Ruminococcus_albu at the species level compared to the Con group (Fig. 4B).

3.4. Differential analysis of fecal metabolites between FDM and Con groups

After quality control, differential metabolites were identified between the FDM group and the Con group using variable importance for the projection (VIP) values of ≥ 1 and $p < 0.05$ as criteria. A total of 41 differential metabolites were detected under both negative (NEG) and positive (POS) modes. Specifically, in comparison to the Con group, 23 metabolites were up-regulated, while 18 were down-regulated in the FDM group. Detailed information about the metabolic products is provided in Table 3.

According to the PCA analysis results, the PCA analysis results reveal a noticeable distinction between the FDM group and the Con group. The metabolites obtained in the negative mode (refer to Fig. 5A) exhibited less dispersion compared to those obtained in the positive mode (Fig. 5B). For the differential metabolites (Top 10, $p < 0.05$, Impact >0), KEGG pathway analysis was conducted, highlighting the most significantly enriched pathways in FDM and Con guinea pigs. The four pathways exhibiting the highest significance were the D-Glutamine and D-glutamate metabolism pathway, as well as the Alanine, aspartate, and glutamate metabolism pathway (Fig. 5C). Correlation analysis was carried out for all the different metabolites, as illustrated in Fig. 6, it can be seen that the most critical metabolite, L-glutamic acid, was significantly positively correlated with 1-Aminocyclopane-1-Carboxylate, Protoporphyrin IX, 4-Hydroxybenzaldehyde, L-Pyroglutamic acid, Oleamide, Azelaic acid, 2-Methylcitrate, and 2-Aminophenol, and was negatively correlated with 7-Oxocholesterol, Genistein, Hexadecanedioic acid, 6-Hydroxynicotinic acid, and Kynurenic acid.

Table 1
Eyeball parameters of guinea pigs before and after experimental induction.

Group	0 week			4 weeks		
	RE(D)	AL(mm)	Vitreous cavity depth(mm)	RE(D)	AL(mm)	Vitreous cavity depth(mm)
Con (n = 10)	3.35 ± 0.38	7.38 ± 0.12	3.24 ± 0.17	2.45 ± 0.77	7.95 ± 0.21	3.42 ± 0.21
FDM(n = 10)	3.08 ± 0.43	7.33 ± 0.12	3.17 ± 0.11	-3.31 ± 1.78	8.41 ± 0.10	3.86 ± 0.16
T	1.53	0.81	0.96	9.38	6.35	5.20
P	0.14	0.43	0.35	<0.0001	<0.0001	<0.0001

Note: Con, control; FDM, form deprivation myopia; RE, refractive error; D, diopter; AL, axial length; P, *p* value; T, *t* value; $p < 0.05$ represents statistically significant difference.
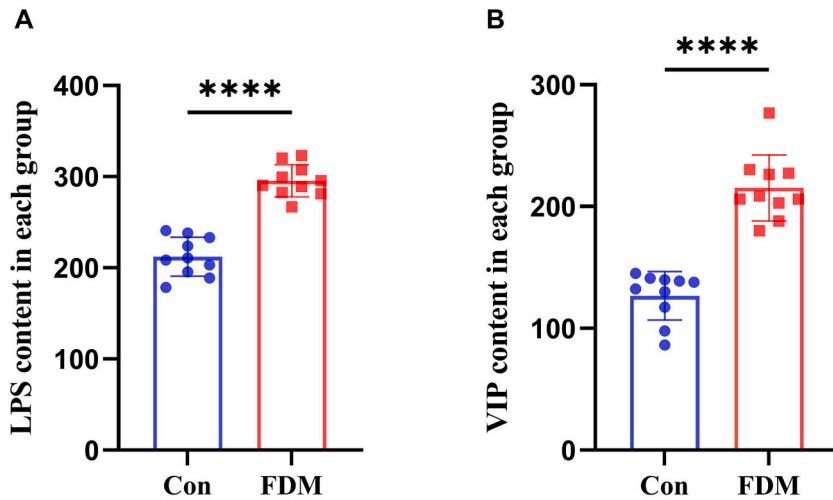
Fig. 1. The concentration of serum VIP and LPS (ng/L). Note: A, results of serum LPS; B, results of serum VIP. Con, control; FDM, form deprivation myopia; LPS, lipopolysaccharide; VIP, vascular active intestinal peptide. ****$p < 0.0001$.
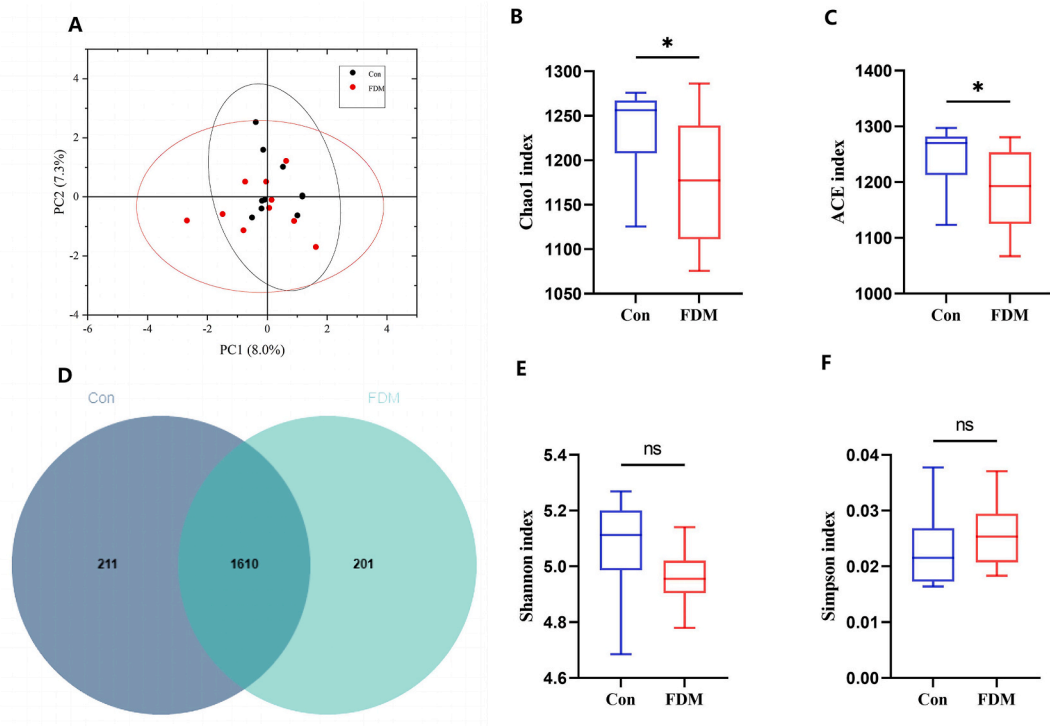

Fig. 2. Differences in diversity and richness of gut microbiota between two groups of guinea pigs. Note: A, PCA analysis of Con and FDM; B. The difference in Chao1 index between the two groups; C. The difference in ACE index between the two groups; D. Venn plots of the abundance of two groups of gut microbiota; E. The difference in Shannon index between two groups; F. The difference in Simpson index between two groups. Con, control; FDM, form deprivation myopia; LPS,lipopolysaccharide; VIP, vascular active intestinal peptide. *$p < 0.05$; ns; the difference is not statistically significant.

3.5. Correlation analysis between differential metabolites, gut microbiota, serum VIP, and LPS between FDM group and Con group

To elucidate the relationships between serum VIP, LPS, and the identified differential biomarkers in FDM and Con groups, Pearson analysis was conducted on gut microbiota, metabolites, VIP, and LPS. Correlation with gut microbiota: VIP, and LPS exhibited a significantly positive correlation with Ruminococcus, Ruminococcus_albus, [Clostridium]_papyrosolvens ($p < 0.05$). Negative
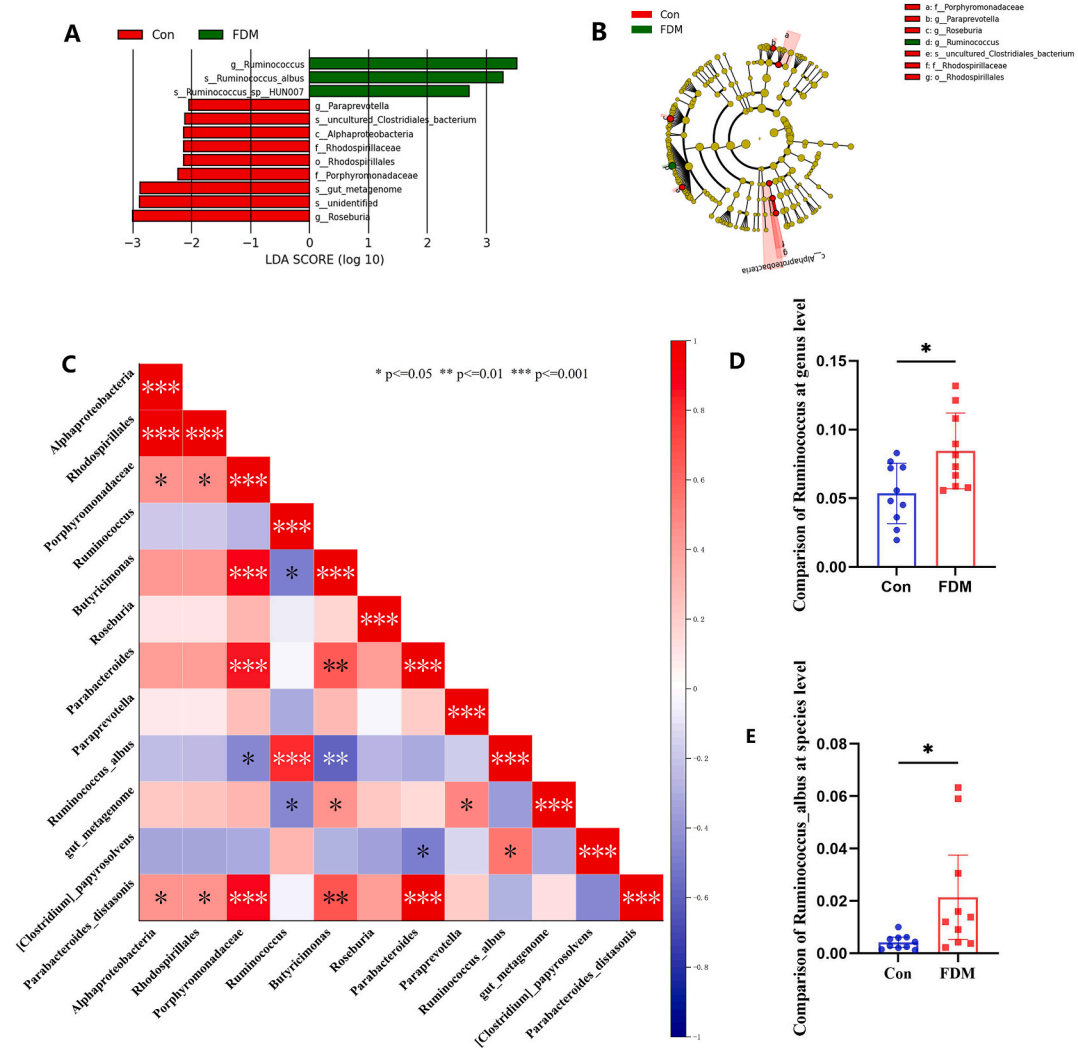
Fig. 3. Differences in gut microbiota between FDM and Con. Note: A, LDA scores (log10) (LDA>2.0) for diverse bacterial taxa between FDM and control guinea pigs under LEfSe analysis; B. Branching plot representing the difference in classification level between FDM and Con generated by LEfSe analysis; C. Correlated heat maps of different intestinal flora; D. Comparison of Ruminococcus at the genus level between FDM and Con; E. Comparison of Ruminococcus_albus at the species level between FDM and Con. Con, control; FDM, form deprivation myopia; LPS, lipopolysaccharide; VIP, vascular active intestinal peptide. *$p < 0.05$; **$p < 0.01$; ***$p < 0.001$.

Table 2
Differential gut microbiota information of FDM compared with Con group.

| No	Name of gut microbiota	Classification level	The average value of Con group (OUTs)	The average value of FDM group (OUTs)	P_Con VS FDM	FDM/ Con
1	Alphaproteobacteria	class	0.001948 ± 0.00	0.0008982 ± 0.00	0.01	Down
2	Rhodospirillales	order	0.001941 ± 0.00	0.0008837 ± 0.00	0.01	Down
3	Porphyromonadaceae	family	0.00415 ± 0.00	0.002733 ± 0.00	0.02	Down
4	Roseburia	genus	0.0153 ± 0.01	0.005579 ± 0.01	0.02	Down
5	Ruminococcus	genus	0.05357 ± 0.02	0.08446 ± 0.03	0.01	Up
6	Butyricimonas	genus	0.001499 ± 0.00	0.0008779 ± 0.00	0.02	Down
7	Parabacteroides	genus	0.001467 ± 0.00	0.0008631 ± 0.00	0.04	Down
8	Paraprevotella	genus	0.001679 ± 0.00	0.0007443 ± 0.00	0.04	Down
9	Ruminococcus_albus	species	0.004205 ± 0.00	0.02142 ± 0.02	0.03	Up
10	gut_metagenome	species	0.01188 ± 0.01	0.005911 ± 0.00	0.01	Down
11	[Clostridium] _papyrosolvens	species	0.004102 ± 0.00	0.007923 ± 0.00	0.03	Up
12	Parabacteroides_distasonis	species	0.001338 ± 0.00	0.0007375 ± 0.00	0.03	Down
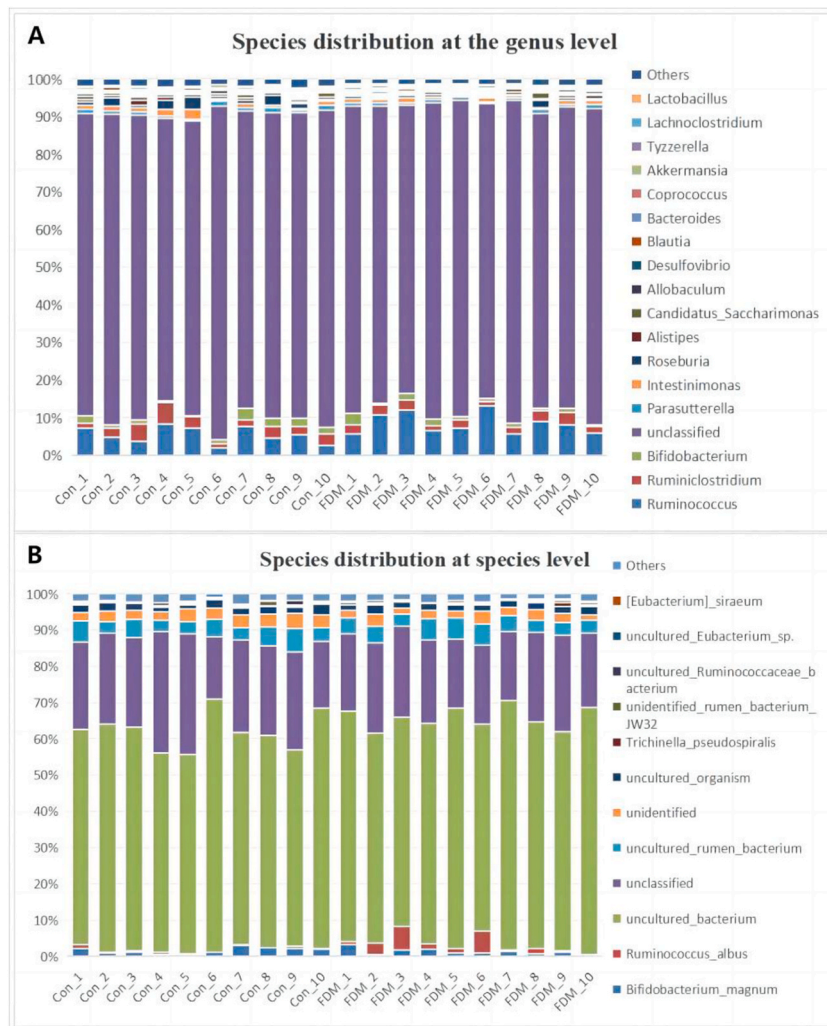
Fig. 4. Results of gut microbiota at genus and species levels in two groups of guinea pigs. Note: A. The results of gut microbiota at the genus level; B. The results of gut microbiota at the species level.

correlations were observed with the remaining gut microbiota ($p < 0.05$), except for VIP and Roseburia (Fig. 7A). Correlation with Metabolites: VIP and LPS showed positive correlations with metabolites such as L-Glutamic acid, Lyso PE, Azelaic acid, 4-Hydroxybenzaldehyde, Protoporphyrin IX, etc. Negative correlations were observed with metabolites like Hexadecanoic acid, CoQ4, 7-Oxocholesterol, 16-Hydroxyhexadecanoic acid, Acetophenone, etc (Fig. 7B). Correlation between metabolites and gut microbiota showed that Ruminococcus_albus exhibited significant correlations with 10 metabolites, being positively correlated with 4-Hydroxybenzaldehyde, 1-Aminocyclopane-1-Carboxylate, L-Glutamic acid, L-Pyroglucamic acid, Ursolic acid, Choline, 6-Hydroxycapric acid, 2-Hydroxyisocapric acid, Lyso PE (15:0/0:0), and Oleamide. Besides, negative correlations were observed with six metabolites of Genistein, CoQ4, 6-Hydroxynicotinic acid, 7-Oxocholesterol, Cholest-4,6-Dien-3-One, and Suberic acid (p < 0.05) (Fig. 7C).

4. Discussion

Microbiomics and metabolomics play pivotal roles in identifying gut microbiota and their corresponding metabolites. The former typically employs 16S rRNA gene sequencing, primarily to evaluate microbiota diversity and abundance [28]. Meanwhile, metabolomics enables the simultaneous detection of overall changes in biological system metabolites, often utilizing LC-MS as a common method for non-targeted metabolite detection [29]. In this study, we adopted a combined approach of 16S rRNA gene sequencing and LC-MS for the first time to detect and compare fecal gut microbiota and metabolites between FDM and Con guinea pigs. Our investigation identified 12 gut microbiota and 41 metabolites as potential biomarkers associated with myopia. Notably, we observed a significant elevation in the abundance of Ruminococcus at the genus level and Ruminococcus_albus at the species level was significantly elevated in the FDM group. Additionally, serum concentrations of VIP and LPS were substantially higher in myopic guinea pigs compared to controls. Furthermore, these elevations showed a positive correlated with Ruminococcus and Ruminococcus_albus

Table 3
Differential metabolite information of FDM compared with Con group

No	Formula	Name	Molecular weight	RT.[min]	VIP	*p* value	Tendency	Mode
1	$C_7H_{10}O_7$	2-Methylcitrate	206.04	1.15	1.12	0.03	Up	NEG
2	$C_{19}H_{40}NO_7P$	Lyso PE(14:0)	425.25	8.42	1.21	0.01	Up	NEG
3	$C_9H_{16}O_4$	Azelaic acid	188.10	4.94	1.24	0.00	Up	NEG
4	$C_{23}H_{42}NO_7P$	Lyso PE(18:3)	475.27	8.63	1.21	0.00	Up	NEG
5	$C_4H_{11}N$	Isobutylamine	73.09	13.21	1.46	0.00	Up	POS
6	$C_4H_7NO_2$	1-Aminocyclopropane-1-Carboxylate	101.05	0.77	1.36	0.00	Up	POS
7	$C_{34}H_{34}N_4O4$	Protoporphyrin IX	562.26	12.91	1.15	0.00	Up	POS
8	$C_7H_6O_2$	4-Hydroxybenzaldehyde	122.038	5.46	1.50	0.00	Up	POS
9	$C_5H_7NO_3$	L-Pyroglutamic acid	129.04	0.78	1.22	0.00	Up	POS
10	$C_{23}H_{44}NO_5P$	Lyso PE(18:2)	477.29	9.23	1.10	0.00	Up	POS
11	$C_{18}H_{38}NO_5P$	Sphingosine 1-Phosphate	379.25	13.77	1.21	0.00	Up	POS
12	$C_{18}H_{35}NO$	Oleamide	281.27	9.87	1.34	0.01	Up	POS
13	$C_5H_9NO_4$	L-Glutamic acid	147.05	0.77	1.13	0.01	Up	POS
14	C_6H_7NO	2-Aminophenol	109.05	0.80	1.41	0.01	Up	POS
15	$C_5H_5NO_2$	Pyrrole-2-carboxylic acid	111.033	1.15	1.20	0.01	Up	POS
16	$C_{33}H_{46}N_4O_6$	Stercobilin	594.34	5.26	1.32	0.02	Up	POS
17	$C_{16}H_{33}NO$	Hexadecanamide	255.26	12.48	1.09	0.02	Up	POS
18	$C_6H_{12}O_3$	2-Hydroxyisocaproic acid	132.08	3.35	1.11	0.02	Up	POS
19	$C_5H_{13}NO$	Choline	103.10	0.73	1.01	0.03	Up	POS
20	$C_6H_{12}O_3$	6-Hydroxycaproic acid	132.08	3.88	1.08	0.03	Up	POS
21	$C_6H_6N_2O_2$	Urocanic acid	138.04	0.79	1.07	0.03	Up	POS
22	$C_{20}H_{42}NO_7P$	Lyso PE(15:0/0:0)	439.27	9.23	1.43	0.04	Up	POS
23	$C_6H_8N_2O_2$	Methylimidazoleacetic acid	140.06	0.76	1.06	0.05	Up	POS
24	$C_6H_5NO_3$	6-Hydroxynicotinic acid	139.03	1.19	1.72	0.03	Down	NEG
25	$C_8H_9NO_4$	4-Pyridoxic acid	183.05	0.81	1.27	0.03	Down	NEG
26	$C_9H_9NO_3$	Hippuric acid	179.06	2.84	1.12	0.02	Down	NEG
27	$C_{16}H_{30}O_4$	Hexadecanedioic acid	286.21	9.40	1.04	0.01	Down	NEG
28	$C_8H_{14}O_4$	Suberic acid	174.09	1.15	1.21	0.01	Down	NEG
29	$C_{20}H_{28}O_2$	Tretinoin	300.21	11.46	1.29	0.01	Down	NEG
30	$C_{15}H_{10}O_5$	Genistein	270.05	5.14	1.30	0.01	Down	NEG
31	$C_{30}H_{48}O_3$	Ursolic acid	456.36	12.44	1.48	0.00	Down	NEG
32	$C_{16}H_{32}O_3$	16-Hydroxyhexadecanoic acid	272.23	9.98	1.33	0.00	Down	NEG
33	$C_{27}H_{42}O$	Cholest-4,6-Dien-3-One	382.33	6.82	1.34	0.00	Down	POS
34	$C_{27}H44O_2$	7-Oxocholesterol	400.34	8.61	1.29	0.00	Down	POS
35	$C_{29}H_{42}O_4$	CoQ4	454.31	11.94	1.52	0.00	Down	POS
36	$C_8H_{11}N$	Phenethylamine	121.09	2.13	1.33	0.00	Down	POS
37	C_8H_8O	Acetophenone	120.06	0.81	1.14	0.01	Down	POS
38	$C_6H_{10}O_4$	Adipic acid	146.06	8.77	1.20	0.01	Down	POS
39	$C_{11}H_{16}N_2O_8$	N-Acetylaspartylglutamic acid	304.09	5.78	1.33	0.01	Down	POS
40	$C_{10}H_7NO_3$	Kynurenic acid	189.04	2.58	1.14	0.03	Down	POS
41	$C_4H_6O_2$	Crotonic acid	86.04	0.75	1.30	0.04	Down	POS

Note: VIP, variable importance for the projection; NEG, negative mode; POS, positive mode.

(Fig. 7A). The detected metabolites were primarily linked to the D-Glutamine and D-glutamate metabolism pathway, as well as the Alanine, aspartate, and glutamate metabolism pathway. Many of these metabolites exhibited close associations with VIP and LPS, unveiling a significant correlation among VIP, LPS, and specific metabolites (Fig. 7B). Moreover, our correlation analysis between metabolites and gut microbiota indicated that differences in metabolites between FDM and Con were associated with distinct abundances of specific gut microbiota (Fig. 7C). Based on these findings, we hypothesize that gut microbiota, their metabolites, as well as VIP and LPS, collectively contribute to the mechanism underlying FDM in guinea pigs.

Moreover, in order to reveal the key relationships between different gut microbiota and different metabolites, we also conducted correlation analysis. And it was found that Ruminococcus-albus was significantly positively correlated with Ruminococcus, [Clostridium] - papyrosolvens, and significantly negatively correlated with Porphyromonadaceae and Butyrisimonas; Besides, the metabolite L-glutamic acid was significantly positively correlated with 1-Aminocyclopane-1-Carboxylate, Protoporphyrin IX, 4-Hydroxybenzaldehide, L-Pyroglutamic acid, Oleamide, Azelaic acid, 2-Methylcitrate, 2-Aminophenol, and negatively correlated with 7-Oxocholesterol, Genistein, Hexadecanedioic acid, 6-Hydroxynicotinic acid, and Kynurenic acid. It can be clearly observed that the correlation changes of these gut microbiota and metabolites in FDM guinea pigs are also consistent with the changes in VIP and LPS, indicating that specific gut microbiota and their metabolites may not act independently and are interrelated to affect changes in the body.

We initially observed a significant increase in the levels of VIP and LPS in the serum of myopic guinea pigs. VIP plays a pivotal role in the regulating microorganisms within the body, contributing notably to maintaining gut microbiota homeostasis [30]. However, its precise involvement in myopia regulation remains contentious. In the study by Cakmak et al. [31], the role of VIP in the FDM model was explored, demonstrating that injecting VIP into the vitreous cavity of FDM chicks prevented myopia occurrence. This finding is consistent with the work of Seltner RL et al., who reported a decrease in FDM following intravitreal injection of porcine VIP as early as 1995 [32]. Conversely, Yiu WC et al. suggested that the VIP gene may not play a significant role in human susceptibility to high myopia
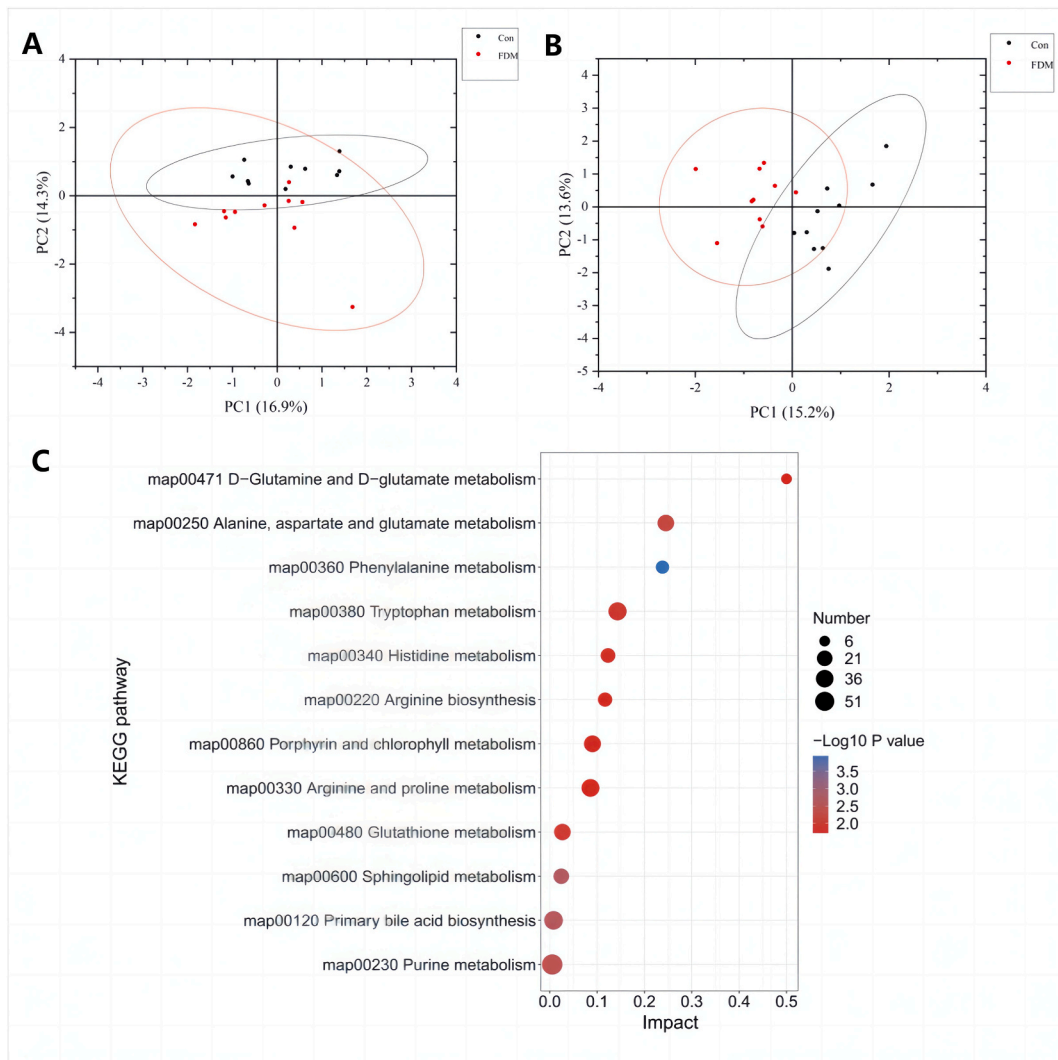
Fig. 5. PCA results of metabolites and KEGG pathway analysis of differential metabolites between FDM and Con group. Note: A. PCA analysis of metabolites in NEG mode; B. PCA analysis of metabolites in POS mode; C. KEGG pathway diagram of differential metabolites (top 10), where the size of the dots represents the number of differential metabolites in the pathway, and the color of the dots represents the -log10(p) value of the hypergeometric test(Larger values represent approximately significant enrichment). Con, control; FDM, form deprivation myopia; NEG, negative; POS, positive; KEGG, Kyoto Encyclopedia of Genes and Genomes. (For interpretation of the references to color in this figure legend, the reader is referred to the Web version of this article.)

[33]. Additionally, Mathis U et al. [34] detected VIP in the retina of FDM mice but found no significant difference between VIP levels in FDM mice and control mice. In our study, we observed a significantly higher concentration of VIP in the serum of FDM guinea pigs compared to non-myopic guinea pigs. Notably, the concentration of VIP was positive correlation with the up-regulated gut microbiota and metabolites expressed in myopic guinea pigs. These discrepant findings could be attributed to variations in animal species and sample collection locations. While our study focused on serum, most other studies concentrated on the retina and sclera.

Additionally, we noted similarities in the changes of LPS in the serum of FDM guinea pigs compared to the Con group, consistent with Lin HJ et al.'s study [35]. Their research demonstrated that injection of monocular form deprivation (MFD) in Syrian hamsters and the inflammatory stimulus LPS promoted the progression of myopia. In our investigation, we observed a close relationship between changes in LPS levels and myopia, particularly in relation to specific gut microbiota and metabolites. LPS, as a metabolic byproduct of microorganisms, mainly consists of lipids and polysaccharides. It is primarily produced by Gram-negative bacteria and serves as a major component of the cell wall, playing a crucial role in maintaining the integrity of the outer membrane permeability barrier and actively participating in host interactions [36]. Given the interplay between VIP, LPS, and microbiota in myopia, our findings suggest the involvement of the eye-gut axis in the pathogenesis of FDM in guinea pigs. Elevated serum levels of VIP and LPS in FDM guinea pigs are associated with alterations in gut microbiota and metabolites, including the increased abundance of Ruminococcus_albus.
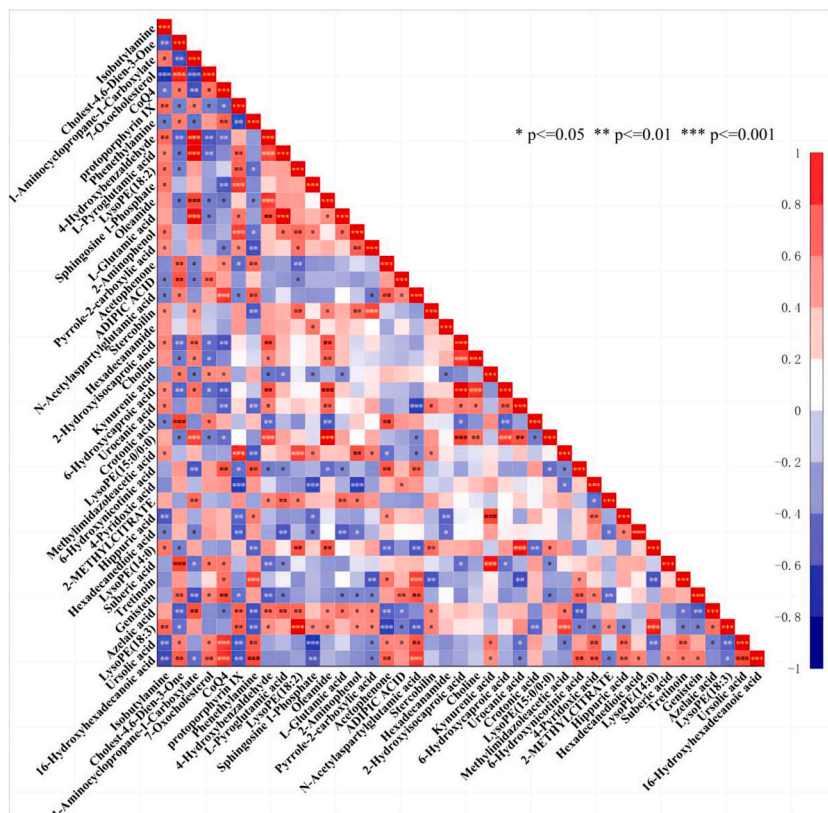
Fig. 6. Correlation heatmap of differential metabolites between FDM group and Con group.

Besides, we noted that Ruminococcus exhibited the most pronounced increase in abundance among the gut microbiota of FDM guinea pigs, particularly with a significant enrichment of Ruminococcus_Albus. Ruminococcus_Albus is extensively studied for its crucial role in fiber degradation, serving as a key member of the rumen community and a major contributor to cellulose breakdown [37]. It secretes highly active cellulase enzymes, facilitating the efficient degradation of microcrystalline cellulose [38,39]. While Ruminococcus_Albus has not been previously reported in association with ophthalmological diseases, studies in neurological diseases suggest potential connections. For example, Choo et al. [40] found evidence suggesting a protective effect of Ruminococcus_Albus on patients with AD. Their experiments using human neuroblastoma SH-SY5Y cells treated with heat-inactivated Ruminococcus_Albus demonstrated inhibition of apoptosis and oxidative stress induced by β-Amyloid protein,a hallmark of AD pathology. Given that AD is characterized by elevated levels of beta-amyloid protein in the brain, resulting in neuronal death and DeoxyriboNucleic Acid (DNA) damage, the researchers proposed that heat-inactivated Ruminococcus_Albus could potentially serve as a probiotic for AD treatment. As highlighted in our introduction, myopia is not solely an ophthalmological condition but also a retinal neurodegenerative disorder. Interestingly, pathological changes in AD align with disease-related alterations in the default mode network center [41]. Additionally, abnormalities in the amplitude of low-frequency fluctuations (ALFFs) of the default brain network have also been demonstrated in myopic patients [42]. Given the significant association of Ruminococcus_Albus with myopia observed in our study, we suggest a potential correlation between AD and myopia, possibly implicating both brain and intestinal microbes. This intriguing hypothesis warrants further investigation to elucidate potential links between these seemingly disparate conditions.

Furthermore, we conducted a comparative analysis of fecal metabolites between myopic and non-myopic guinea pigs, revealing significant alterations in 41 metabolites, including L-glutamate, in the myopic group. KEGG pathway analysis of these metabolites indicated their involvement primarily in the regulation of amino acid metabolic pathways, particularly the glutamic acid metabolic pathway, which is consistent with our observation of a significant increase in L-glutamate levels in the FDM group. Moreover, we observed a positive correlation between Ruminoccus_Albus and not only VIP and LPS but also with L-Glutamic acid. L-glutamic acid is a well-established excitatory neurotransmitter widely distributed in the brain and spinal cord, formed after the decarboxylation of Glutamate. In contrast,γ-Aminobutyric acid (GABA), serves as an inhibitory neurotransmitter. Both Glutamic acid and GABA play crucial roles as neurotransmitters in the retina and are implicated in the development of myopia. Guoping et al. [43] conducted a study on guinea pigs using a lens-induced myopia (LIM) model, where they assessed the ratio of Glutamic acid to GABA (RGG) levels in the retina. Their findings revealed higher RGG levels in myopic patients compared to the control group, indicating a positive correlation. This aligns with our results demonstrating an up-regulation of fecal L-Glutamic acid in FDM guinea pigs. Although reports on statistically significant differences in metabolites related to myopia between FDM and control guinea pigs are limited (except for L-Glutamic
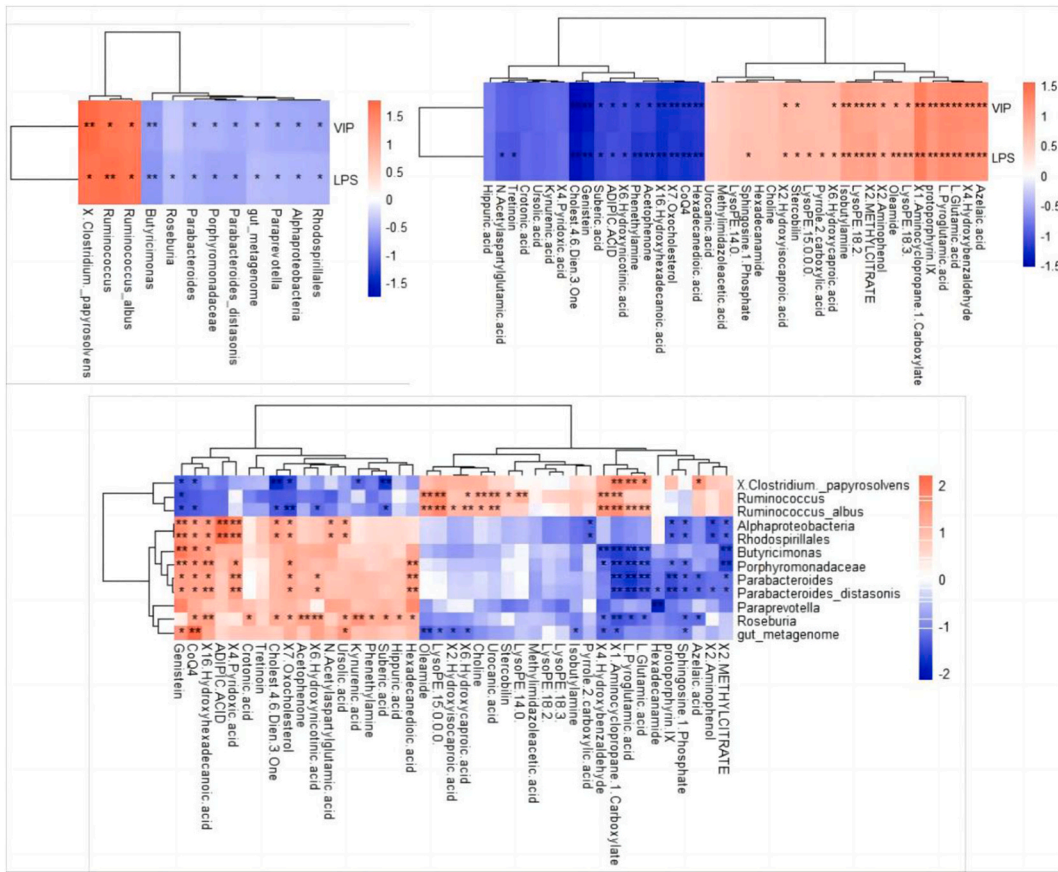
Fig. 7. Heat map of correlation between VIP, LPS, metabolites and gut microbiota. Note: A. The association between VIP, LPS and gut microbiota; B. The association between VIP, LPS and metabolites; C. The association between metabolites and gut microbiota; LPS,lipopolysaccharide; VIP, vascular active intestinal peptide. Red represents positive correlation, blue represents negative correlation. *$p < 0.05$; **$p < 0.01$. (For interpretation of the references to color in this figure legend, the reader is referred to the Web version of this article.)

acid), our KEGG metabolic pathway analysis suggests the potential involvement of L-glutamic acid in the mechanism of myopia. This involvement may occur through its influence on the metabolic pathways of glutamine and D-glutamate metabolism, as well as the alanine, aspartate, and glutamate metabolism pathway. Further exploration of the specific roles and interactions of these pathways could offer valuable insights into the mechanisms underlying myopia development in guinea pigs.

Indeed, microbiomics technology plays a crucial role in unraveling the gut-eye axis in eye diseases. Myopia stands out as one of the most prevalent ophthalmic conditions [44]. Despite its prevalence, studies investigating the role of gut microbes in myopia remain scarce. Xi et al. [45] conducted a review on the association between myopia and gut microbiota. At the time, research reports on gut microbiota and myopia were virtually non-existent. They proposed that the pathological conditions of gut microbiota contributing to myopia may primarily involve tissue ischemia and hypoxia, changes in dopamine levels, and inflammatory reactions. Additionally, they hypothesized that alterations in gut microbiota could potentially trigger the onset of myopia. Currently, research on the relationship between myopia and gut microbiota is largely limited to studies by Li et al. [46], who utilized microbiome techniques to identify differences in gut microbiota between myopic and non-myopic mice. Their findings indicated a significant decrease in the relative abundance of Firmicutes and an increase in Actinobacteria in the gut of myopic mice, suggesting alterations in gut microbiota composition. However, Li et al. acknowledged that differences exist between their animal model and the human body, emphasizing the need for further research to validate changes in gut microbiota in myopic patients. Discrepancies in gut microbiota findings between our study and that of Li et al. may stem from differences in animal species. Nonetheless, both studies highlighted the potential involvement of amino acid metabolism pathways in myopia. Specifically, myopic mice exhibited significant changes in glutamine and D-glutamic acid metabolism, as well as alanine, aspartic acid, and glutamic acid metabolism pathways, consistent with our research findings. However, it's worth noting that while we observed a significant increase in L-glutamic acid concentration in FDM guinea pigs, Li et al. reported a decrease in L-glutamic acid concentration in myopic mice. This disparity could be attributed to the different sample types analyzed, guinea pig feces in our study versus mouse serum in theirs. Further research is warranted to validate differences in gut microbiota composition and metabolites in myopic guinea pigs. In conclusion, while existing studies shed light on the potential role of gut microbiota in myopia, more research is needed to elucidate the intricate mechanisms underlying this relationship, especially in diverse animal models and human subjects.

In summary, our study utilizing the FDM guinea pig model revealed a significant association between myopia and VIP, LPS, as well as gut microbiota and their metabolites. However, it's essential to acknowledge several limitations inherent in our study. Due to constraints in the laboratory environment, our animals were housed in an SPF environment rather than a sterile one. Despite this, we timplemented stringent measures to ensure the sterility of the experiment, such as providing sterile food and water. Fecal sample collection was conducted using high-pressure steam sterilization to enhance asepsis. Additionally, we maintained a consistent feeding environment for all guinea pigs. These precautions were implemented to minimize potential sources of contamination and maintain the reliability of our experimental conditions.

5. Conclusion

In conclusion, our study indicates that FDM guinea pigs display heightened serum levels of VIP and LPS, accompanied by potential modifications in gut microbiota composition. Particularly, Ruminococcus_Albus appears significantly enriched in fecal samples, alongside increased levels of metabolites like L-Glutamic acid. The observed positive correlation among VIP, LPS, and Ruminococcus_Albus suggests a plausible association between systemic inflammatory factors and alterations in gut microbiota during myopia. Moreover, our findings suggest a potential role of L-Glutamic acid in myopia pathogenesis, potentially mediated through the regulation of Glutamic and D-Glutamate metabolism pathways, as well as the Alanine, aspartate, and Glutamate metabolism pathways. Nonetheless, it's imperative to acknowledge the need for further research to validate and elaborate on our proposed hypothesis.

Ethics statement

This study was reviewed and approved by Shanghai Aier Eye Animal Ethics Committee, with the approval number: No. SHAIER2023YN002. All animals in this study were approved by the Institutional Animal Care and Use Committee (IACUC) of WestChina-Frontier Pharma Tech Co., Ltd. (Approval Number: IACUC- SW-S2023023-P001-02), and comply with Animal Research: Reporting in Vivo Experiments (ARRIVE) guidelines.

Data availability

Data will be made available on request.

Declaration of competing interest

The authors declare that they have no known competing financial interests or personal relationships that could have appeared to influence the work reported in this paper.

Appendix. ASupplementary data

Supplementary data to this article can be found online at https://doi.org/10.1016/j.heliyon.2024.e30491.

References

[1] E.D. Leon, M.P. Francino, Roles of secretory immunoglobulin a in host-microbiota interactions in the gut ecosystem, Front. Microbiol. 13 (2022) 880484, https://doi.org/10.3389/fmicb.2022.880484.
[2] J.L. Floyd, M.B. Grant, The gut-eye axis: lessons learned from murine models, OPHTHALMOL, THER 9 (3) (2020) 499–513, https://doi.org/10.1007/s40123-020-00278-2.
[3] Y. Zhang, X. Zhou, Y. Lu, Gut microbiota and derived metabolomic profiling in glaucoma with progressive neurodegeneration, Front. Cell. Infect. Microbiol. 12 (2022) 968992, https://doi.org/10.3389/fcimb.2022.968992.
[4] E.V. Gart, J.S. Suchodolski, T.J. Welsh, R.C. Alaniz, R.D. Randel, S.D. Lawhon, Salmonella typhimurium and multidirectional communication in the gut, Front. Microbiol. 7 (2016) 1827, https://doi.org/10.3389/fmicb.2016.01827.
[5] L. Ibanez, M. Rouleau, A. Wakkach, C. Blin-Wakkach, Gut microbiome and bone, Joint Bone Spine 86 (1) (2019) 43–47, https://doi.org/10.1016/j.jbspin.2018.02.008.

[6] G. Sharon, T.R. Sampson, D.H. Geschwind, S.K. Mazmanian, The central nervous system and the gut microbiome, Cell 167 (4) (2016) 915–932, https://doi.org/10.1016/j.cell.2016.10.027.

[7] D.C. Zysset Burri, S. Morandi, E.L. Herzog, L.E. Berger, M.S. Zinkernagel, The role of the gut microbiome in eye diseases, Prog. Retin. Eye Res. 92 (2023) 101117, https://doi.org/10.1016/j.preteyeres.2022.101117.

[8] P. Napolitano, M. Filippelli, S. Davinelli, S. Bartollino, R. Dell'Omo, C. Costagliola, Influence of gut microbiota on eye diseases: an overview, Ann. Med. 53 (1) (2021) 750–761, https://doi.org/10.1080/07853890.2021.1925150.

[9] X. Bai, Q. Xu, W. Zhang, C. Wang, The gut-eye axis: correlation between the gut microbiota and autoimmune dry eye in individuals with sjogren syndrome, Eye Contact Lens 49 (1) (2023) 1–7, https://doi.org/10.1097/ICL.0000000000000953.

[10] G. Chisari, E.M. Chisari, A.M. Borzi, C.G. Chisari, Aging eye microbiota in dry eye syndrome in patients treated with enterococcus faecium and saccharomyces boulardii, Curr. Clin. Pharmacol. 12 (2) (2017) 99–105, https://doi.org/10.2174/1574884712666170704145046.

[11] J. Hu, C. Wang, X. Huang, et al., Gut microbiota-mediated secondary bile acids regulate dendritic cells to attenuate autoimmune uveitis through tgr5 signaling, Cell Rep. 36 (12) (2021) 109726, https://doi.org/10.1016/j.celrep.2021.109726.

[12] S. Kodati, H.N. Sen, Uveitis and the gut microbiota, Best Pract. Res. Clin. Rheumatol. 33 (6) (2019) 101500, https://doi.org/10.1016/j.berh.2020.101500.

[13] K. Liu, J. Zou, H. Fan, H. Hu, Z. You, Causal effects of gut microbiota on diabetic retinopathy: a mendelian randomization study, Front. Immunol. 13 (2022) 930318, https://doi.org/10.3389/fimmu.2022.930318.

[14] J. Chen, D.F. Chen, K.S. Cho, The role of gut microbiota in glaucoma progression and other retinal diseases, Am. J. Pathol. 193 (11) (2023) 1662–1668, https://doi.org/10.1016/j.ajpath.2023.06.015.

[15] K. Socala, U. Doboszewska, A. Szopa, et al., The role of microbiota-gut-brain axis in neuropsychiatric and neurological disorders, Pharmacol. Res. 172 (2021) 105840, https://doi.org/10.1016/j.phrs.2021.105840.

[16] M. Hirayama, K. Ohno, Parkinson's disease and gut microbiota, Ann. Nutr. Metab. 77 (Suppl 2) (2021) 28–35, https://doi.org/10.1159/000518147.

[17] C. Jiang, G. Li, P. Huang, Z. Liu, B. Zhao, The gut microbiota and alzheimer's disease, J. Alzheimers Dis. 58 (1) (2017) 1–15, https://doi.org/10.3233/JAD-161141.

[18] M. Pan, F. Zhao, B. Xie, et al., Dietary omega-3 polyunsaturated fatty acids are protective for myopia, Proc. Natl. Acad. Sci. U.S.A. 118 (43) (2021), https://doi.org/10.1073/pnas.2104689118.

[19] C. Chen, C. Wang, X. Zhou, et al., Nonsteroidal anti-inflammatory drugs for retinal neurodegenerative diseases, Prostag. Other Lipid Mediat. 156 (2021) 106578, https://doi.org/10.1016/j.prostaglandins.2021.106578.

[20] X. Wang, C. Yu, X. Liu, et al., Fenofibrate ameliorated systemic and retinal inflammation and modulated gut microbiota in high-fat diet-induced mice, Front. Cell. Infect. Microbiol. 12 (2022) 839592, https://doi.org/10.3389/fcimb.2022.839592.

[21] K. Li, Q. Wang, L. Wang, Y. Huang, Cognitive dysfunctions in high myopia: an overview of potential neural morpho-functional mechanisms, Front. Neurol. 13 (2022) 1022944, https://doi.org/10.3389/fneur.2022.1022944.

[22] S. Chaudhary, S.S. Kumaran, V. Goyal, et al., Cortical thickness and gyrification index measuring cognition in parkinson's disease, Int. J. Neurosci. 131 (10) (2021) 984–993, https://doi.org/10.1080/00207454.2020.1766459.

[23] Y.J. Wu, N. Wu, X. Huang, et al., Evidence of cortical thickness reduction and disconnection in high myopia, Sci. Rep. 10 (1) (2020) 16239, https://doi.org/10.1038/s41598-020-73415-3.

[24] S.I. Said, V. Mutt, Polypeptide with broad biological activity: isolation from small intestine, Science 169 (3951) (1970) 1217–1218, https://doi.org/10.1126/science.169.3951.1217.

[25] M. Bains, C. Laney, A.E. Wolfe, et al., Vasoactive intestinal peptide deficiency is associated with altered gut microbiota communities in male and female c57bl/6 mice, Front. Microbiol. 10 (2019) 2689, https://doi.org/10.3389/fmicb.2019.02689.

[26] J. Troger, G. Kieselbach, B. Teuchner, et al., Peptidergic nerves in the eye, their source and potential pathophysiological relevance, Brain Res. Rev. 53 (1) (2007) 39–62, https://doi.org/10.1016/j.brainresrev.2006.06.002.

[27] J. Rymer, C.F. Wildsoet, The role of the retinal pigment epithelium in eye growth regulation and myopia: a review, Vis. Neurosci. 22 (3) (2005) 251–261, https://doi.org/10.1017/S0952523805223015.

[28] A. Regueira-Iglesias, C. Balsa-Castro, T. Blanco-Pintos, I. Tomas, Critical review of 16s rrna gene sequencing workflow in microbiome studies: from primer selection to advanced data analysis, Mol. Oral Microbiol. 38 (5) (2023) 347–399, https://doi.org/10.1111/omi.12434.

[29] L. Cui, H. Lu, Y.H. Lee, Challenges and emergent solutions for lc-ms/ms based untargeted metabolomics in diseases, Mass Spectrom. Rev. 37 (6) (2018) 772–792, https://doi.org/10.1002/mas.21562.

[30] A.C. Ericsson, M. Bains, Z. McAdams, J. Daniels, S.B. Busi, J.A. Waschek, G.P. Dorsam, The G protein-coupled receptor, VPAC1, mediates vasoactive intestinal peptide-dependent functional homeostasis of the gut microbiota, Gastro Hep. Adv. 1 (2) (2022) 253–264, https://doi.org/10.1016/j.gastha.2021.11.005.

[31] A.I. Cakmak, H. Basmak, H. Gursoy, et al., Vasoactive intestinal peptide, a promising agent for myopia? Int. J. Ophthalmol. 10 (2) (2017) 211–216, https://doi.org/10.18240/ijo.2017.02.05.

[32] R.L. Seltner, W.K. Stell, The effect of vasoactive intestinal peptide on development of form deprivation myopia in the chick: a pharmacological and immunocytochemical study, Vis. Resour. 35 (9) (1995) 1265–1270, https://doi.org/10.1016/0042-6989(94)00244-g.

[33] W.C. Yiu, M.K. Yap, W.Y. Fung, P.W. Ng, S.P. Yip, Genetic susceptibility to refractive error: association of vasoactive intestinal peptide receptor 2 (vipr2) with high myopia in chinese, PLoS One 8 (4) (2013) e61805, https://doi.org/10.1371/journal.pone.0061805.

[34] U. Mathis, F. Schaeffel, Glucagon-related peptides in the mouse retina and the effects of deprivation of form vision, Graefes Arch. Clin. Exp. Ophthalmol. 245 (2) (2007) 267–275, https://doi.org/10.1007/s00417-006-0282-x.

[35] H.J. Lin, C.C. Wei, C.Y. Chang, et al., Role of chronic inflammation in myopia progression: clinical evidence and experimental validation, EBioMedicine 10 (2016) 269–281, https://doi.org/10.1016/j.ebiom.2016.07.021.

[36] C. Whitfield, M.S. Trent, Biosynthesis and export of bacterial lipopolysaccharides, Annu. Rev. Biochem. 83 (2014) 99–128, https://doi.org/10.1146/annurev-biochem-060713-035600.

[37] G.I. Rozman, G. Yin, I. Borovok, et al., Functional phylotyping approach for assessing intraspecific diversity of ruminococcus albus within the rumen microbiome, FEMS Microbiol. Lett. 362 (3) (2015) 1–10, https://doi.org/10.1093/femsle/fnu047.

[38] S. Koike, Y. Kobayashi, Development and use of competitive pcr assays for the rumen cellulolytic bacteria: fibrobacter succinogenes, ruminococcus albus and ruminococcus flavefaciens, FEMS Microbiol. Lett. 204 (2) (2001) 361–366, https://doi.org/10.1111/j.1574-6968.2001.tb10911.x.

[39] K.D. Kohl, A.W. Miller, J.E. Marvin, R. Mackie, M.D. Dearing, Herbivorous rodents (neotoma spp.) Harbour abundant and active foregut microbiota, Environ. Microbiol. 16 (9) (2014) 2869–2878, https://doi.org/10.1111/1462-2920.12376.

[40] S. Choo, M. An, Y.H. Lim, Protective effects of heat-killed Ruminococcus albus against β-amyloidInduced apoptosis on SH-SY5Y cells, J. Microbiol. Biotechnol. 34 (1) (2024) 85–93, https://doi.org/10.4014/jmb.2308.08045.

[41] E. Bruner, J.M. de la Cuetara, M. Masters, H. Amano, N. Ogihara, Functional craniology and brain evolution: from paleontology to biomedicine, Front. Neuroanat. 8 (2014) 19, https://doi.org/10.3389/fnana.2014.00019.

[42] X.W. Zhang, R.P. Dai, G.W. Cheng, W.H. Zhang, Q. Long, Altered amplitude of low-frequency fluctuations and default mode network connectivity in high myopia: a resting-state fmri study, Int. J. Ophthalmol. 13 (10) (2020) 1629–1636, https://doi.org/10.18240/ijo.2020.10.18.

[43] L. Guoping, Y. Xiang, W. Jianfeng, et al., Alterations of glutamate and gamma-aminobutyric acid expressions in normal and myopic eye development in Guinea pigs, Invest. Ophthalmol. Vis. Sci. 58 (2) (2017) 1256–1265, https://doi.org/10.1167/iovs.16-21130.

[44] T.V. Tkatchenko, A.V. Tkatchenko, Pharmacogenomic approach to antimyopia drug development: pathways lead the way, Trends Pharmacol. Sci. 40 (11) (2019) 833–852, https://doi.org/10.1016/j.tips.2019.09.009.

[45] X. Xi, L. Han, M. Ding, et al., Exploring the relationship between intestinal flora and the pathological mechanism of myopia in adolescents from the perspective of Chinese and western medicine: a review, Medicine (Baltimore) 102 (12) (2023) e33393, https://doi.org/10.1097/MD.0000000000033393.

[46] H. Li, S. Liu, K. Zhang, X. Zhu, J. Dai, Y. Lu, Gut microbiome and plasma metabolome alterations in myopic mice, Front. Microbiol. 14 (2023) 1251243, https://doi.org/10.3389/fmicb.2023.1251243.